AGU100 ADVANCING EARTH AND SPACE SCIENCE

JGR

Journal of Geophysical Research: Earth Surface

RESEARCH ARTICLE
10.1029/2017JF004499

Geometric Controls on Tidewater Glacier Retreat in Central Western Greenland

G. A. Catania[1,2], L. A. Stearns[3], D. A. Sutherland[4], M. J. Fried[1,2], T. C. Bartholomaus[5], M. Morlighem[6], E. Shroyer[7], and J. Nash[7]

[1]Institute for Geophysics, University of Texas at Austin, Austin, TX, USA, [2]Department of Geosciences, University of Texas at Austin, Austin, TX, USA, [3]Department of Geology, University of Kansas, Lawrence, KS, USA, [4]Geological Sciences, University of Oregon, Eugene, OR, USA, [5]Department of Geological Sciences, University of Idaho, Moscow, ID, USA, [6]Earth System Science, University of California, Irvine, CA, USA, [7]College of Earth, Ocean, and Atmospheric Sciences, Oregon State University, Corvallis, OR, USA

Key Points:
- Glacier termini in central West Greenland began progressive retreat in 1998 +/-3 years
- Heterogeneous retreat rates and extents can be partially explained by local differences in bed topography
- Length of overdeepening behind the terminus controls the amount of retreat observed

Supporting Information:
- Supporting Information S1
- Movie S1
- Movie S2
- Movie S3

Correspondence to:
G. A. Catania,
gcatania@ig.utexas.edu

Citation:
Catania G. A., Stearns, L. A., Sutherland, D. A., Fried, M. J., Bartholomaus, T. C., Morlighem, M., et al. (2018). Geometric controls on tidewater glacier retreat in central western Greenland. *Journal of Geophysical Research: Earth Surface*, *123*, 2024–2038. https://doi.org/10.1029/2017JF004499

Received 15 SEP 2017
Accepted 11 JUN 2018
Accepted article online 19 JUN 2018
Published online 30 AUG 2018

Abstract Glacier terminus changes are one of the hallmarks of worldwide glacier change, and thus, there is significant focus on the controls and limits to retreat in the literature. Here we use the observational record of glacier terminus change from satellite remote sensing data to characterize glacier retreat in central West Greenland with a focus on the last 30 years. We compare terminus observations of retreat to glacier/fjord geometry from available bed and bathymetry data and find that glacier retreat accelerates through wide, overdeepened parts of the bed characterized by retrograde bed slopes. We find that the morphology of the overdeepening can be used as a predictive measure for the length of retreat and that short regions (less than twice the seasonal change in terminus position) of the bed with prograde bed slopes are not sufficient to stop a retreating terminus. Even narrow overdeepenings can control glacier retreat, likely because they focus subglacial runoff, which entrains warm water in the fjords when it emerges at the grounding line and melts the terminus, creating enhanced local retreat. Future retreat of these glaciers is assessed given upstream fjord geometry.

Plain Language Summary Glaciers that reach the marine margin of the Greenland Ice Sheet are experiencing increases in mass loss over time. These losses are greater than land-terminating glaciers and are spatially variable. Even glaciers that drain into the same fjord system can experience different amounts, rates, and durations of retreat and thinning. To explain this, we examined retreat over an ~30-year record derived from satellite images of Greenland and compared it to the submarine fjord and subglacial topography across a region containing 15 glaciers. We find good correspondence between glacier retreat and the length of an overdeepened reach of the fjord behind the glacier terminus.

1. Introduction

Understanding the controls on the mass balance of the Greenland Ice Sheet has been an intense focus of research over the last decade, with importance placed on improving our understanding of how the ocean controls the dynamics of marine-terminating outlet glaciers. This priority has been motivated by the recent, large, and rapid increases in mass loss observed for many tidewater (or ocean-terminating) glaciers that drain Greenland (e.g., Larsen et al., 2016, Moon et al., 2012, Velicogna et al., 2014). Indeed, present-day rates of tidewater glacier mass losses are larger than losses for their land-terminating counterparts and larger than losses that occurred during the 1930s, when the Arctic experienced increases in air temperature similar to today (Bjørk et al., 2012). The different behavior of marine-terminating and land-terminating glaciers suggests that the atmosphere does not directly drive present-day losses of tidewater glaciers alone and that their interaction with the ocean plays an important role in controlling recent changes.

Superimposed on the observed trend of ice sheet-wide tidewater glacier mass loss acceleration is a pattern of heterogeneous mass loss between glaciers that remains largely unexplained. All aspects of tidewater glacier dynamics exhibit spatiotemporal variability including changes in ice surface elevation (Csatho et al., 2014; Felikson et al., 2017), ice speed (Bevan et al., 2012; Joughin et al., 2010; Moon et al., 2012), and terminus position (Bevan et al., 2012; Moon & Joughin, 2008; Motyka et al., 2017; Murray et al., 2015). Together, these factors add complexity to the ice sheet-wide mass loss signal (e.g., Chen et al., 2011, Larsen et al., 2016). Many studies use the presence of such variability to suggest that there is no simple control on tidewater glacier dynamics that is applicable for all glaciers (Carr, Stokes, & Vieli, 2013; Carr, Vielli, & Stokes, 2013; McFadden et al., 2011; Murray et al., 2015; Schild & Hamilton, 2013).

The terminus region of marine-terminating outlet glaciers represents the region where the ice sheet, ocean, and atmosphere act together through a suite of processes to influence glacier behavior. Several mechanisms have been proposed as controls on tidewater glacier terminus position including (1) ambient melting at the glacier terminus from warm water in the fjord in contact with the ice face (Carroll et al., 2016; Chauché et al., 2014); (2) enhanced melt induced by mixing of buoyant subglacial discharge with deep, warm fjord waters (Carroll et al., 2016; Chauché et al., 2014; Motyka et al., 2003; Straneo et al., 2010); (3) weakening of iceberg melange or sea ice (Bevan et al., 2012; Cassotto et al., 2015; Howat et al., 2010; Moon et al., 2015; Robel, 2017); and (4) increased sliding due to increases in meltwater lubrication at the bed (De Juan et al., 2010; Moon et al., 2015), although this last mechanism appears to be more important at subannual time scales (Carr, Stokes, & Vieli, 2013). All of these mechanisms can act in concert, via regional changes to climate, to initiate retreat of glaciers. However, the synchronous timing of multiple processes obscures a clear interpretation of how glaciers respond dynamically to climate.

Tidewater glaciers are also controlled by subglacial topography, because glacier geometry controls the state of stress at the terminus (Bassis, 2013; Pfeffer, 2007; van der Veen, 1996). This idea has been investigated intensively on marine-terminating glaciers in Alaska where overdeepenings and/or fjord widenings have been found to be associated with faster rates of retreat (McNabb & Hock, 2014; Meier & Post, 1987; Mercer, 1961). Additional studies have examined the role of topography in controlling glacier retreat in Greenland (Carr et al., 2015; Lüthi et al., 2016; Warren, 1991; Warren & Glasser, 1992), Antarctica (e.g., Seroussi et al., 2017), the Russian Arctic (e.g., Carr et al., 2014), Patagonia (Aniya et al., 1997), and Svalbard (e.g., Błaszczyk et al., 2013). However, many of these studies focus on single glacier systems largely due to the lack of offshore bathymetry data in many fjords and poorly constrained bed topography at the glacier terminus, where thick, warm, and heavily crevassed ice limits the utility of ice-penetrating radars. As a result, model studies are used to confirmed that topography plays a key role in modulating the glacier dynamic response (Choi et al., 2017; Enderlin et al., 2013; Jamieson et al., 2012; Morlighem et al., 2016; Nick et al., 2007).

Here we present a detailed overview of the impact of fjord topography on glacier retreat rates for 15 glaciers over the last 30 years in central west Greenland. Our goal in this paper is twofold. First, we aim to examine long-term changes in terminus position in order to identify the timing of retreat, which may reveal a common forcing mechanism. Second, we aim to compare patterns of retreat to fjord topography to assess its control on retreat once initiated. Termini for glaciers in this region have been studied by several previous authors (Bevan et al., 2012, Howat et al., 2010; Lüthi et al., 2016; McFadden et al., 2011; Moon & Joughin, 2008; Murray et al., 2015; Rignot, Xu, et al., 2016; Rignot, Fenty, et al., 2016), and Moon and Joughin (2008) identified that increases in air temperature were correlated to retreat onset after 2000. However, no clear mechanism has yet been identified to explain divergent patterns of retreat across regions of glaciers here, or elsewhere. In addition, while most authors point out that glacier/fjord geometry is a likely control on the pattern of retreat, only Lüthi et al. (2016) provide a detailed comparison between retreat and fjord topography to demonstrate this.

Our analysis augments the existing glacier terminus history with an examination of fjord and glacier topography across a broad region. This is made possible through surveys of glaciated valleys and fjords in this region in Greenland (Rignot, Fenty, et al., 2016; Studinger et al., 2010) and mass-conservation techniques that improve estimates of bed topography at glacier termini (Morlighem et al., 2017), where data are most limited. By examining the relationship between bed geometry and retreat for an entire region, we are able to provide a more comprehensive, observationally based understanding of the role of topography in glacier retreat. In particular, we examine the bed slope at the terminus at the time of retreat and the role of topographic sills in controlling the pace of retreat.

2. Data and Measurements

Our region of interest (ROI) spans 15 tidewater glaciers that drain a portion of central west Greenland (Figure 1) and includes glaciers that vary in catchment area, grounding line ice thickness (Carroll et al., 2016), decadal changes in ice thickness (Csatho et al., 2014; Felikson et al., 2017), velocity (Joughin et al., 2010), seasonal changes in velocity (Moon et al., 2012), and changes in terminus position (Murray et al., 2015) over time and space (Table 1).

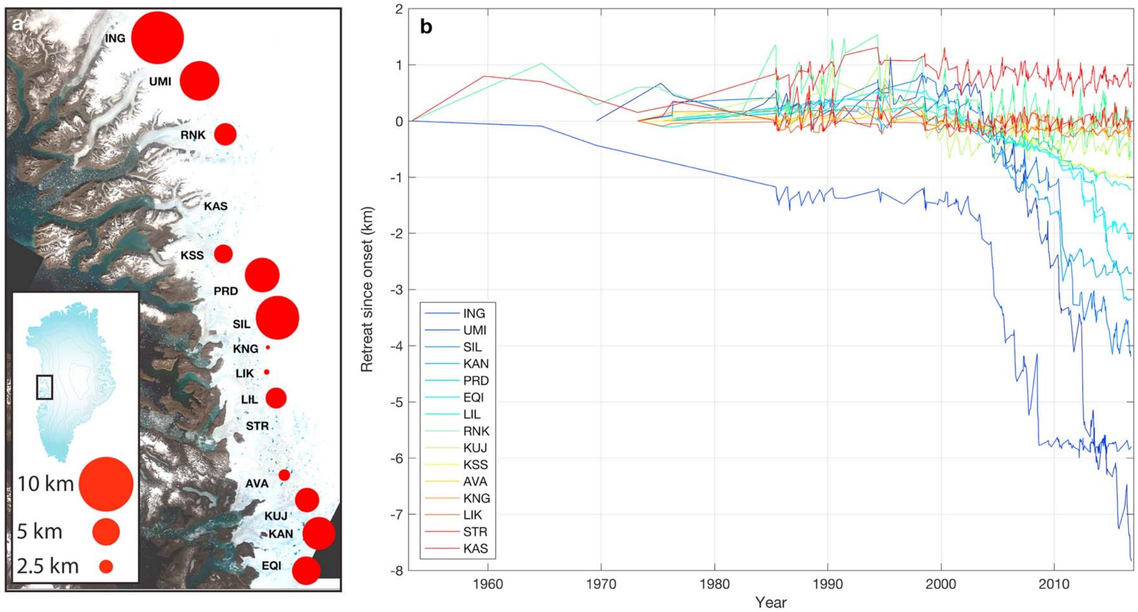

Figure 1. (a) Location of the 15 glaciers in our region of interest. The red circles indicate the change in terminus length observed since the time of progressive retreat onset. Glaciers without red circles (KAS and STR) are not retreating. (b) Time series of glacier termini in the region relative to their position at the time of progressive retreat onset. Glaciers are listed in order of decreasing retreat with blue indicating the greatest total retreat and red indicating the most stable. Full form of glacier names are provided in Table 1.

2.1. Terminus Traces

Glacier termini are manually digitized from several satellite sensors. The bulk of the terminus traces (up to 95% for some glaciers) come from Landsat, operating from 1970 to present day, but we also include images from Corona from the 1950s and 1960s, Advanced Spaceborne Thermal Emissions and Reflection Radiometer from 2000 to 2010, and TerraSar-X, which launched in 2007. We have chosen to end our data set after the melt season of 2016. The sampling frequency for each of these satellites differs, but in general, acquisition has been more frequent since the late 1990s when Landsat-7 was launched. The presence of clouds and data gaps obscures portions of glacier termini sporadically. Despite these limitations, we obtain a mean of 357 terminus traces for each of the 15 glaciers in our ROI with ~12 traces per year before 1999 and ~19 traces per year after 1999. While we present data from earlier observations for context, our analysis is limited to the time period from 1985 to 2016 because of the increased frequency of observations. Seasonally, we have roughly double the number of terminus traces in the summer than in the winter. We provide the terminus data for all glaciers in the supporting information but use one glacier Umiamako Isbrae (UMI) in the main text as an illustrative example. UMI underwent a large ~4-km retreat beginning in 2001 and ending in 2008, and recent bathymetric surveys have improved our understanding of the shape of the submarine fjord (Rignot, Fenty, et al., 2016).

We determine the average terminus position by projecting equally spaced points along a single glacier terminus trace (an average of ~100 points are picked for each glacier terminus) to the glacier centerline and computing the mean location of these points along the centerline. Our method is a variation of the Bow method implemented by Bjørk et al. (2012). We also examined terminus changes computed using the curvilinear box method following Moon and Joughin (2008) and found no significant differences in the terminus positions over time. Comparison of these and various other methods for tracking terminus change by Lea et al. (2017) suggested that the choice of method results in minimal (<20%) differences. Given our focus on the long-term nature of terminus change where retreats exceed 1 km, small differences between method choice are within the fluctuations of seasonal terminus changes, and thus, we feel justified in our choice of method.

The long-term trend in terminus position is isolated from seasonal variations by interpolating onto a 15-day time interval and applying a locally weighted linear regression filter over a 4-year time span (e.g., Figure 2). Retreat rates are calculated by taking the time derivative of the smoothed record (e.g., Figure 2). We then use the standard deviation of the difference between the terminus position and the smoothed terminus position from 1999 to 2016 (when sampling frequency is highest) to quantify the mean seasonality of the terminus

Table 1
Tidewater Glacier Characteristics for Glaciers in Central West Greenland

Glaciers	Catchment area (km^2)	Mean grounding line depth (m)	Terminus speed (km/year)	Mass change (Gt)
Retreating glaciers				
Ingia Isbræ (ING)	2.7×10^3	130	1.6	−3.87
Sermeq Silardleq (SIL)	7.9×10^3	341	2.8	−14.5
Umiamiko Isbræ (UMI)	2.5×10^3	264	1.3	−13.1
Perdlerfiup Sermia (PRD)	8.0×10^2	78.1	0.39	−1.94
Kangilerngata Sermia (KAN)	2.3×10^3	260	1.4	−9.84
Eqip Sermia (EQI)	3.0×10^4	24.7	1.6	−4.15
Sermeq Kujatdleq (KUJ)	5.3×10^1	372	3.7	−0.941
Rink Isbræ (RNK)	3.9×10^4	555	4.2	0.214
Lille Glacier (LIL)	3.2×10^2	40.1	0.64	−0.713
Kangerluarsuup Sermia (KSS)	7.1×10^2	76.1	0.3	−1.90
Sermeq Avangnardleq (AVA)	3.3×10^3	178	1.6	0.645
Sermilik (LIK)	1.7×10^2	62.2	1.3	−0.078
Kangilleq (KNG)	1.8×10^2	173	1.2	−0.421
Stable glaciers				
Store Gletscher (STR)	3.1×10^5	328	5.0	2.10
Kangerdlugssup Sermerssua (KAS)	3.4×10^3	211	2.0	3.78

Note. Catchment area is estimated using the Greenland Ice Mapping Project Digital Elevation Model (Howat et al., 2014). Mean grounding line depth is given as an average mean grounding line depth for all termini in 2016. Terminus speed is the mean speed in 2016. Mass change between 1985 and 2013 (Felikson et al., 2017).

position. This metric for seasonality is used as an estimate of the uncertainty in our measurements of total retreat (Table 2).

All of the glaciers in our ROI exhibit seasonal retreats, during the summer and fall. We define the onset of *progressive terminus retreat* from the terminus position time series by identifying when the terminus retreats in a given summer more than it did the previous two summers. The first summer of progressive retreat is then the time that long-term retreat began (Table 2 and Figure 2). For glaciers with smaller total retreats and large seasonal variation in terminus position, the exact timing of progressive retreat onset is difficult to detect. This is exacerbated by reduced Landsat imagery availability between 1994 and 1999 when progressive retreat onset began for most glaciers. To provide a check on identification of the timing of progressive retreat onset, we also examine the change in curvature of the smoothed terminus position and look for times when the retreat rate exhibits positive trends. These results are indistinguishable from our initial pick of progressive retreat onset. The total amount of retreat is calculated for each glacier by estimating the difference between the mean terminus position in the year of progressive retreat onset and the mean in terminus position during the last year of observations from the unsmoothed terminus record (Table 2). In a similar fashion, slowing or termination of retreat can be identified where the average terminus position remains in the same location for >2 years causing retreat rates to drop to ~0 (e.g., ~2009 in Figure 2).

2.2. Ice Speed

Width-average glacier terminus speed comes from a compilation of publicly available data sets where ice velocity is derived from optical (Fahnestock et al., 2016; Howat, 2017; Rosenau et al., 2015) and radar (Joughin et al., 2010) data. We apply the same smoothing technique as described for the terminus change time series to the velocity time series over the time period where data are available to examine changes in velocity on time scales longer than seasonal time scales (Figure 2).

2.3. Fjord Geometry

Topographic characteristics of the glacier fjords come from merged data of seafloor bathymetry and glacier bed elevation data using the mass-conservation approach to determine bed topography in areas where data are missing (here called MCBed, Morlighem et al., 2017). Under the ice sheet, the bed elevation is constrained by available radar-derived ice thickness observations (see references in Morlighem et al., 2017). Since the MCBed uses velocity data from 2008 to 2009 to solve for bed topography beneath the ice sheet, bed

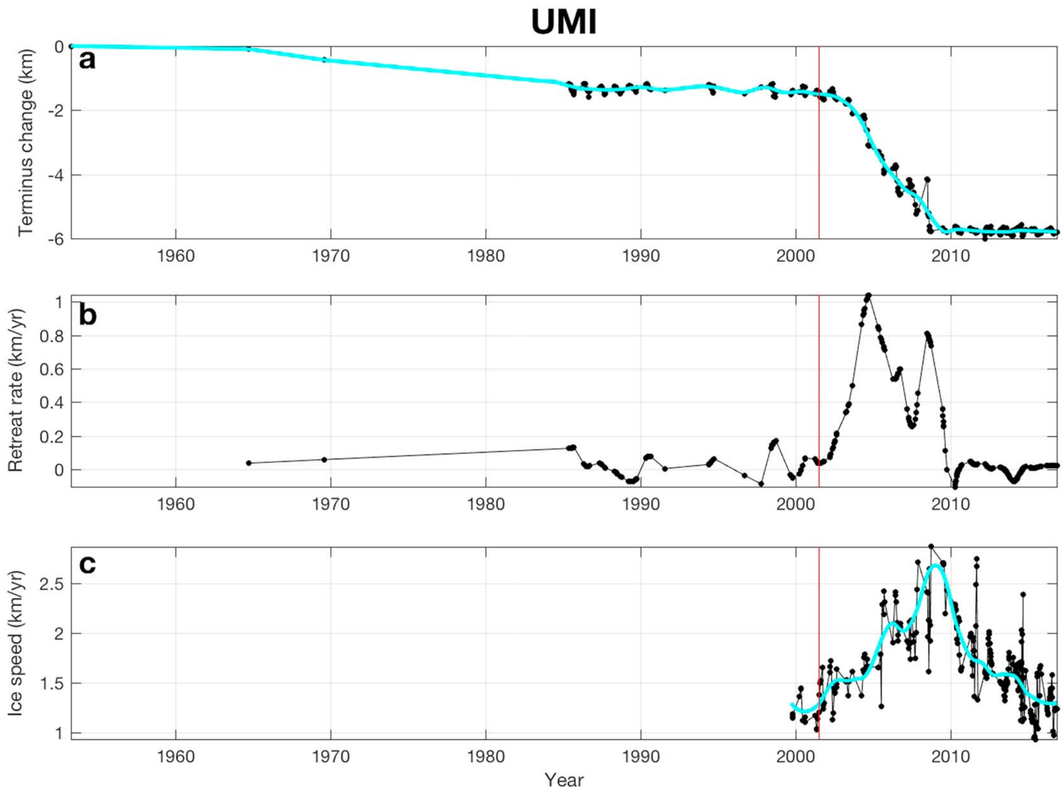

Figure 2. (a) Observed retreat of Umiamiko Glacier terminus. Mean terminus position (black) and smoothed terminus position with locally weighted scatterplot smoothing filter applied (blue). (b) Retreat rate for Umiamiko calculated as the time derivative of the smoothed terminus position. (c) Ice speed for UMI (black) and smoothed ice speed (blue). Red line in each panel indicates the chosen date of progressive progressive retreat onset described in the text.

topography is computed up to the terminus positions in that same year, even if the glaciers have subsequently retreated. Comparison of radar data used to constrain the MCBed solution and the MCBed shows that MCBed consistently underestimates the bed elevation (supplementary information figures) but does a good job of reproducing the shape of the bed. Since the bed shape determines bed slope, we argue that MCBed-determined bed slopes are adequate for interpreting the influence of bed slope on glacier terminus retreat.

Bathymetry data for the MCBed comes from multiple sources (see references in Morlighem et al., 2017) and for 10 glaciers (UMI, RNK, KSS, PRD, KNG, LIK, KAN, EQI, KAS, and STR) in our ROI fjord bathymetric data extend to the 2016 glacier terminus (Table 2). This provides continuous topographic data to constrain the MCBed solution for 67% in our ROI. For the remaining five glaciers (ING, LIL, KUJ, SIL, and AVA) MCBed solutions are only reliable upstream of the 2008/2009 terminus position, where MCBed is constrained with available radar data. For these glaciers, topography seaward of the 2008/2009 terminus position is estimated based on a natural neighbor interpolation along the fjords (Morlighem et al., 2017). Since we do not think fjord topography seaward of the 2008/2009 terminus position is well constrained in MCBed where fjord bathymetry data are not available, we focus on interpreting terminus change in relation to fjord geometry upstream of the 2008/2009 terminus location for these five glaciers (fjord geometry calculated seaward of the 2008/2009 terminus locations are shown as dotted lines in the supporting information figures). Fjord walls were traced by taking advantage of the Landsat thermal band and using images from late summer in 2015 to thermally differentiate between glacier, ocean, and land. This has the advantage of determining fjord wall locations in shaded regions where the glacier boundaries are optically obscured.

In order to evaluate the influence of fjord geometry on terminus position, we constrain several aspects of the fjord geometry from MCBed including fjord width, depth, bed slope, and submarine cross-sectional area. These variables are measured in two ways: (1) along fjord, extending several kilometers both upstream and downstream of the available terminus observations, and (2) at terminus, extracted at the locations of each

Table 2
Tidewater Glacier Retreat Characteristics Including Retreat Amount (Given as a Length and Total Area Change), Amount of Seasonal Terminus Change Observed From 1999 to 2016, and Timing of Retreat Onset

Glaciers	Retreat (km) [area lost (km^2)]	Seasonality (km)	Time of retreat onset
Retreating glaciers			
Ingia Isbræ (ING)[a]	8.47 [30.9]	±0.355	2002.4
Sermeq Silardleq (SIL)[a]	5.05 [18.9]	±0.215	1998.2
Umiamiko Isbræ (UMI)	4.36 [13.4]	±0.392	2001.5
Perdlerfiup Sermia (PRD)	3.56 [9.33]	±0.096	1998.5
Kangilerngata Sermia (KAN)	2.65 [10.9]	±0.200	1998.5
Eqip Sermia (EQI)	2.54 [9.65]	±0.099	1998.6
Sermeq Kujatdleq (KUJ)[a]	1.80 [8.91]	±0.224	1995.2/1998.4
Rink Isbræ (RNK)	1.53 [7.40]	±0.354	1994.4/1998.3
Lille Glacier (LIL)[a]	1.48 [2.92]	±0.050	1998.4
Kangerluarsuup Sermia (KSS)	1.11 [3.33]	±0.035	1998.3
Sermeq Avangnardleq (AVA)[a]	0.64 [3.38]	±0.057	1995.2/1998.5
Sermilik (LIK)	0.25 [0.37]	±0.067	1995.5
Kangilleq (KNG)	0.23 [0.59]	±0.138	1995.0
Stable glaciers			
Store Gletscher (STR)	−0.01 [−0.02]	±0.175	N/A
Kangerdlugssup Sermerssua (KAS)	−0.56 [−2.14]	±0.168	N/A

[a]Glaciers marked with an asterisk do not have sufficient bathymetry data at their preretreat termini locations.

terminus trace. The former technique allows us to compare glaciers that have undergone significant retreat to those that have not, and the latter technique allows us to examine changes in fjord parameters that occur with time as the terminus moves. Across-fjord observations of fjord geometry are obtained by extracting MCBed data from several hundred cross sections that span across each fjord with a nominal spacing of ~50 m (e.g., Figure 3). Cross sections are oriented near parallel to the glacier termini. Across-fjord width is taken as the distance between the intersection of each fjord wall with each cross section. Fjord depth is extracted from MCBed along each cross section and is used to compute the maximum and mean fjord depth for each cross section. Submarine cross-sectional area is computed as the area enclosed by the fjord depth along each cross section and sea level. All across-fjord geometry (width, mean and maximum fjord depth, and fjord cross-sectional area) are then projected to the glacier centerline in order to get a sense of how these geometry values vary along-fjord. While the bed data are not very noisy, we still smooth along-fjord values over a 500-m distance prior to computing bed slope to ensure that bed slope is also smooth. The mean fjord bed slope is obtained from the smoothed along-fjord mean depth by calculating the gradient in mean fjord depth along-fjord (Figure 3 and supporting information figures). Retrograde (negative) bed slopes deepen up fjord toward the glacier and prograde (positive) bed slopes shallow up fjord toward the glacier. We note that for many glaciers the terminus width did not change significantly over the observational period, somewhat limiting a reliable examination of its relative influence on terminus position. As a result, we do not consider changes in across-fjord width other than within the examination of changes in submarine fjord area.

For at-terminus bed data we simply extract the MCBed data at each point along the terminus trace (e.g., Figure 4) and use these data to obtain the mean and maximum fjord depths for a given terminus trace. Fjord cross-sectional area is computed as the area enclosed by the fjord depth along any terminus trace and sea level. At-terminus bed slope is computed by extracting the along-fjord bed slope (described above) where each terminus trace intersects the along-flow centerline. At-terminus fjord width is computed as the straight line distance between the intersection points of each terminus trace with the fjord wall traces.

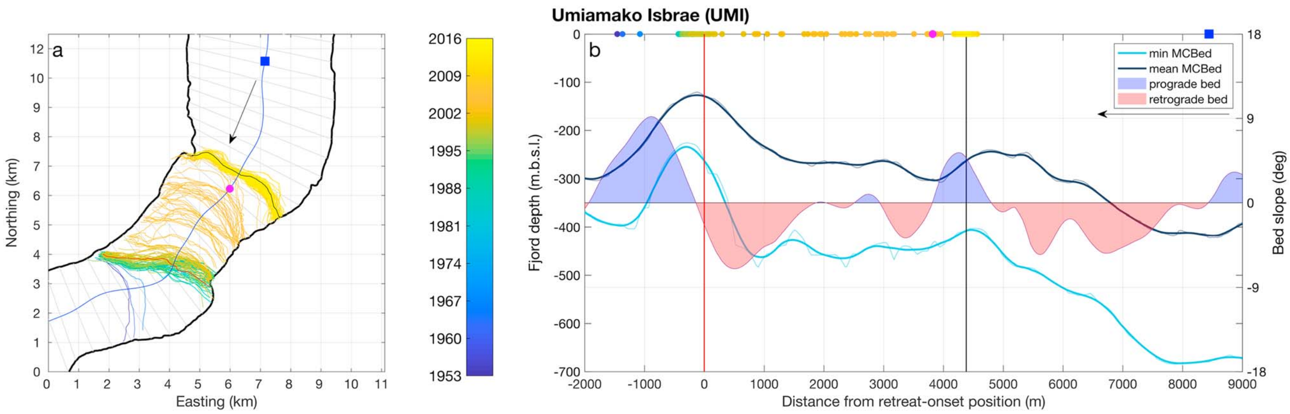

Figure 3. (a) Fjord boundaries (bold black lines), fjord cross sections (gray lines—every 25th cross section shown) where along-fjord geometry is computed, centerline (blue), and terminus positions colored by time. The pink circle indicates the upstream extent of the overdeepening (as measured by overdeepening length, given in the text) from the terminus position at the time of progressive retreat onset (red terminus trace). The blue square indicates the location on the centerline of the predicted future terminus position given the overdeepening length behind the present-day terminus. The black terminus trace indicates the last observed terminus position. (b) Minimum and mean fjord depth below sea level (smoothed and unsmoothed) and mean bed slope shown with terminus positions through time at the top. The shaded line is bed slope derived from the smoothed mean bed depth. The red (blue) shaded regions are retrograde (prograde) bed slope. The vertical red line indicates terminus position at the time of progressive retreat onset. The black line indicates the last observed terminus position. The pink circle indicates the end of the overdeepening behind the terminus at the time of progressive retreat onset. The blue square is the end of the overdeepening behind the last terminus position.

3. Results

3.1. Progressive Retreat Onset

From the beginning of the available observations until the mid-1990s, eight glaciers (53%) in the ROI (EQI, ING, KUJ, LIL, PRD, RNK, SIL, and AVA) underwent small amounts (<500 m) of terminus advance, most noticeable in those glaciers with the smallest seasonal variations in terminus position (Table 2 and supporting information figures). After the mid-1990s, 13 of the 15 glaciers in our ROI (87%) experienced measurable, progressive terminus retreat, that is, in amounts larger than those due to seasonal changes (Figure 1 and Table 2). It is not possible to identify the exact time of progressive retreat onset because of seasonal swings in the terminus position and the sampling frequency of the data, which is worse for some glaciers in the mid-1990s. As a result, the timing provided in our results is an estimate of when retreat began. For the majority of the retreating glaciers, retreat began between 1995 and 1998, but for UMI and ING, retreat began slightly later, in 2001 and 2002, respectively (Table 2 and Figure 2, and supporting information figures). Retreat was clearly underway for most glaciers by 2000, as there was at least a decade of stability prior to this most recent period of retreat. Further, the rate of retreat since the late 1990s is notable in its pace with retreat rates in excess of several hundred meters per year observed for many glaciers. The entire region lost a total glacier surface area of ~120 km^2 as of 2016, with 72% of the loss coming from five glaciers (ING, UMI, SIL, KAN, and PERD; Table 2). Two glaciers (STR and KAS) have not undergone retreat that is detectable outside their range of seasonal variability.

3.2. Retreat Variability in Time and Space

While progressive retreat onset is near coincident across the region, there is considerable heterogeneity in retreat magnitude, duration, and rate between glaciers with no obvious subregional pattern (Figure 1) other than the two northern glaciers initiating retreat a few years later than the rest. Many glaciers have stopped retreating within the observational period. However, unlike the consistent timing of progressive retreat onset, retreat stops or slows at a range of different times. LIK, KNG, and KUJ all stopped in ~2000, UMI stopped in 2008, and KAN stopped in 2010 (Table 2 and supporting information figures). KSS, PRD, and SIL may have also stopped but did so only very recently and so more monitoring would be needed to confirm this; KSS and SIL both stopped in 2015, and PRD stopped in 2016 (Table 2 and supporting information figures).

In addition to regional differences between glaciers, we also observe that many glaciers (ING, PRD, EQI, SIL, KSS, and KAN) experience variations in retreat rate over time (supporting information figures). In these glaciers the fastest rates of retreat occur several years after the onset of retreat, typically when the terminus reaches an area with deeper bed topography (supporting information figures). We note that these are also the glaciers that have undergone the most retreat, which may indicate that retreat rate variability is common, but only seen when a glacier retreats significantly. This could be an observational limitation to the present study and

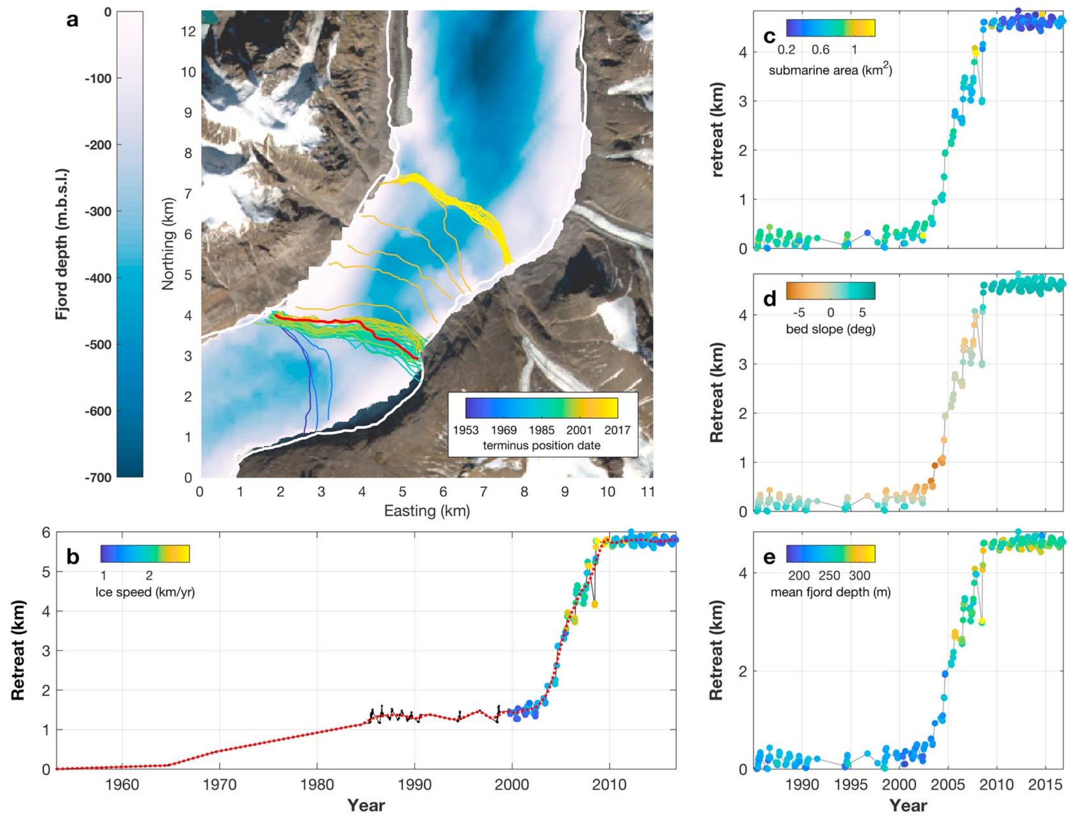

Figure 4. (a) Merged mass-conservation bed and bathymetry data for UMI (blue colormap) overlain with terminus traces. Every tenth terminus trace is shown after 1999 for clarity. The red terminus trace indicates the terminus at the time of progressive retreat onset. Landsat image in background showing fjord walls (white lines). (b) Terminus position over time for all of observational period (black) and smoothed terminus position with locally weighted scatterplot smoothing filter applied (red dashed line). Available ice speed data are shown in color map. Terminus position with time from 1985 to 2016 day shaded by at-terminus mean fjord submarine area (c), mean along-fjord bed slope in degrees (d), and mean fjord depth (e).

others that do not have a sufficiently long enough time period with which to examine terminus changes. Further, this may explain why understanding climatic controls on glacier retreat are so problematic. Neighboring glaciers may experience the same climate, which pushes them into a state of retreat, but have different topography, which modulates the pace of retreat over time. We also observe that the magnitude of retreat is heterogeneous across the terminus face for any given glacier, indicating that processes responsible for retreat can act at specific locations along the terminus. This produces more rapid retreat for some parts of the terminus and thus changes in the terminus shape through time. This is most obvious for KSS and EQI (Lüthi et al., 2016; Figures S12 and S41 and Movies S2 and S3 in the supporting information), but generally most glaciers appear to have more flat or convex termini when they are stable (e.g., STR and KAS) and more concave termini shapes when they are retreating (e.g., UMI and SIL).

3.3. Topography and Retreat

All fjords exhibit complex topography containing sills (local bedrock protrusions or moraines deposited during past glacier standstills), overdeepenings, and numerous smaller bumps and depressions (Figures 3, 4, and supporting information figures). Of the eight glaciers with continuous fjord geometry data across all terminus observations and experiencing progressive retreat onset, all of them had topographic overdeepenings behind the glacier terminus at the time of progressive retreat onset. In several cases (PRD, KNG, KAN, and EQI) the terminus at progressive retreat onset was located seaward of the downstream sill defining the overdeepening and thus in an area with a prograde bed slope. However, we note that the distance from the terminus position at progressive retreat onset to the stoss side of the sill (where the bed is retrograde) is typically short or less than twice the mean seasonal amplitude of the terminus position. Further, supporting the notion that bed geometry controls retreat, the two stable glaciers (KAS and STR) terminate on prograde bed slopes and have fjord constrictions behind their terminus positions that extend several kilometers upstream (Figures S11 and S29).

Topography also appears to exert control on the extent of glacier retreat. Many glaciers (KNG, UMI, KSS, KUJ, and LIK) stop retreating when the terminus encounters a region of the fjord with a prograde bed slope. For example, this occurred for UMI in 2009, when the terminus had retreated nearly 4 km (Figure 3). In addition, a few glaciers (e.g., AVA and ING) are currently still retreating through regions of the fjord with retrograde bed slopes. Confounding this are a few glaciers that have stopped retreating despite being grounded on retrograde bed slopes (e.g., KAN and SIL) and other glaciers that retreated or are still retreating over prograde bed slopes (EQI, LIL, RNK, and PRD). For KAN, the terminus may be stuck in a small constriction on the northern side of the fjord preventing further retreat. SIL has only recently stopped retreating and may continue to retreat in the future. PRD may have recently stopped but retreated over an extensive region with a prograde bed slope. EQI, LIL, and RNK are all retreating very slowly at present (within the noise of seasonal terminus changes), making it difficult to ascertain if topography is truly making a difference on the terminus position.

4. Discussion

4.1. Timing of Progressive Retreat Onset

The timing of glacier retreat in this region is comparable to the timing of retreat for other glaciers across Greenland (Carr et al., 2015; Larsen et al., 2016), in particular, Jakobshavn Isbrae, just south of the ROI, which began its retreat in 1997 (Joughin et al., 2008) and glaciers in the Upernavik region, north of our ROI, which began retreating in the late 1990s (Larsen et al., 2016). Holland et al. (2008) and Motyka et al. (2011) noted that the retreat of Jakobshavn was coincident with a step-change increase in deep ocean temperatures, which was used to implicate ocean forcing as a mechanism to initiate retreat. Warmer ocean temperatures at depth along the western coast of Greenland have been noted by others (Gladish et al., 2015; Myers & Ribergaard, 2013) and are likely in response to shifts in various climate modes operating in the North Atlantic (e.g., Atlantic Multidecadal Oscillation) combined with recent, long-term warming (Straneo & Heimbach, 2013) resulting in a northward diversion of deep, warm water along the western coast of Greenland. Moored observations from the fjords in front of RNK, KAS, and UMI indicate the presence of Atlantic water in these fjords below depths of 300 m (Bartholomaus et al., 2016). Since these glaciers are situated in the northern end of our ROI, we make the assumption that the Atlantic water is present in every fjord in this study below a depth of 300 m. It is possible that a delay in the northward transport of Atlantic Water could explain the observed several year delay in progressive retreat onset for ING and UMI, the northernmost two glaciers in the ROI.

Air temperatures in Greenland have also warmed since the 1970s with mean summer air temperature anomalies above 0 °C since the late 1990s (Bevan et al., 2012; Mernild et al., 2011; van Angelen et al., 2014) driving increased rates of runoff to the ocean and across tidewater glacier termini (van Angelen et al., 2014). Recently, Nöel et al. (2017) identified 1997 as a tipping point in accelerated runoff from Greenland due to the decline of refreezing of meltwater within the firn column. Combined with warmer ocean temperatures at depth, increased runoff will accelerate terminus melt via a buoyant meltwater plume as subglacial discharge entrains warm water at depth bringing it in contact with the terminus (Carroll et al., 2016; Fried et al., 2015; Jenkins, 2011; Motyka et al., 2003). This process is important for all glaciers, including thin ones that terminate in shallow fjords where plumes maintain contact with the terminus face for the entire depth producing equivalent melt rates compared to deeper fjords (Carroll et al., 2016). Rignot, Xu, et al. (2016) found that glacier retreat for several glaciers in our ROI initiated with a near doubling in melt due to this process since the 1990s.

4.2. Changes in Velocity and Terminus Position

The processes that control calving rates and terminus position are disputed, with the central issue being whether flow acceleration causes glacier retreat, or whether glacier retreat causes flow acceleration (Benn et al., 2007). Several studies using observational data and numerical models of tidewater glaciers suggest that enhanced calving triggers a dynamic change in flow speed and ice thickness, which rapidly propagates up glacier (e.g., Howat et al., 2005; Meier & Post, 1987; Nick et al., 2010, 2009). Other studies suggest that acceleration may be initiated by changes in ice rheology and basal sliding, and increased calving is simply a consequence of up-flow acceleration (e.g., Bevan et al., 2015; Luckman et al., 2006; Thomas et al., 2003; van der Veen et al., 2011). This motivated us to explore the relationship between glacier velocities and terminus change in our ROI.

For the glaciers in our ROI, there are no velocity data available prior to ~1999 (with the exception of EQI; Lüthi et al., 2016) and so we are not able to examine changes in velocity due to the onset of progressive long-term retreat. We can, however, determine if glaciers changed velocity in response to changes in terminus position subsequent to 1999; however, no clear relationship between velocity and changes in terminus position emerges. Postretreat increases in glacier speed would be an expected response due to steepening of the glacier surface and a subsequent adjustment in the force balance. Observations of elevation changes for these glaciers suggest that those undergoing retreat have all steepened (Felikson et al., 2017). Some glaciers do exhibit near-coincident changes in speed that appear to be associated with changes in retreat rates (both increases and decreases in retreat rate). For example, UMI had preretreat speeds of ~1.2 km/year that doubled in speed during retreat (Figure 2) but speeds began decreasing back to preretreat values once UMI stopped retreating in 2008. Lüthi et al. (2016) found that velocity for EQI remained relatively unchanged until 2010, when the glacier underwent an enhanced period of retreat.

Nevertheless, there are many glaciers in the ROI that do not show a direct relationship between an increase in retreat rates and an increase in velocities and this suggests that the force-balance adjustment to retreat may be complex. For example, KAN undergoes a large increase in speed from 2005 to 2010 during a period of rapid retreat, but high speeds are more or less sustained even after the terminus stabilized in 2010. Further, this increase in KAN may, in some way, be related to the resumption of flow after a near shutdown in ice speed in 2005–2006 for unknown reasons. Similarly, ING has slowed since 2011 despite experiencing ongoing retreat through the end of the record in 2016 (S1). SIL experiences virtually no change in velocity even though it has undergone a 4-km retreat, with an acceleration in retreat in 2010. PRD also maintains a relatively stable speed during retreat, but it does eventually appear to slow in 2015 when retreat may have stopped. We also observe changes in ice speed at times when terminus positions are relatively stable. From 2000 to 2016, both KNG and KUJ slowed by ~25% and ~38%, respectively, despite stable termini during this time (Figures S19 and S34). Finally, we also observe rapid, single-year slow downs for both AVA and KAS that appear to be unrelated to terminus position or retreat rate. AVA has two of these events in 2004 and 2016, while KAS has these events more frequently in 2008, 2011, 2013, and 2015. These observations suggest that there is a complex relationship between terminus position and velocity.

4.3. Topographic Control on Retreat

Glacier retreat initiated for all glaciers in 1998 ±3 years. While there is some heterogeneity in the onset of retreat through the region, given the range of glacier characteristics, the size of the area covered, and the reduction in sampling frequency in the terminus record in the late 1990s, retreat is essentially near-synchronous through the region. Regionally coincident glacier retreat cannot be initiated because of bed conditions alone; some external force must push the glacier termini to locations where retreat is favorable. Indeed, it may be possible that the range of retreat onset times indicates that some glaciers may have needed a bigger push than others, perhaps due to bed conditions. When we examine the terminal bed geometry for those glaciers that clearly retreated in 1998, we find that they all had terminated in regions of the bed with positive bed slopes (with the exception of KSS). Further, LIK and KNG, which clearly retreated a few years earlier, in 1995, were terminated in regions of the bed with negative bed slopes (supplementary information figures). This suggests that some of the difference in timing of retreat onset may be due to subtleties in the position of the terminus at the time when regional retreat began.

While regional ocean and air temperature changes in the late 1990s appear responsible for pushing the glaciers in this region into an initial state of retreat, the pace and duration of retreat since then are more closely tied to fjord geometry. Several previous authors have suggested that as a grounding line retreats into deeper water, ice discharge increases leading to a feedback that further accelerates retreat on theoretical grounds (Meier & Post, 1987; Schoof, 2007; Thomas & Bentley, 1978; Weertman, 1974) and observational evidence (Larsen et al., 2016; McNabb & Hock, 2014; Motyka et al., 2017; Pfeffer, 2007; Post et al., 2011; Warren, 1991). We find that the amount of retreat is related to the length of the overdeepening behind the terminus at retreat onset, which can be estimated by measuring the distance over which the bed slope remains retrograde behind the terminus (Figure 5). Supporting this is the observation that both of the stable glaciers (STR and KAS) sit on prograde bed slopes that extend up glacier from the 2016 terminus ~2 and 1.5 km, respectively. Similar broad sills may be responsible for the relatively stability of other glaciers in Greenland when compared to their neighbors. For example, Motyka et al. (2017) show a broad sill for a glacier with limited retreat and a narrow sill for a neighboring glacier with much more extensive retreat in Greenland.

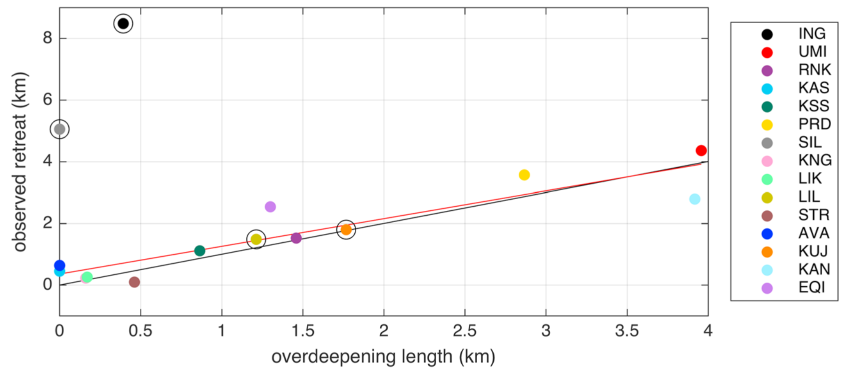

Figure 5. Overdeepening length upstream of the terminus at the time of progressive retreat onset plotted against total retreat observed since progressive retreat onset. Points outlined with black circles have poorly constrained MCBed solutions at progressive retreat onset locations. The black line gives the 1:1 relationship. The red line shows a linear regression using only glaciers well constrained with MCBed. The R^2 value of the linear regression is 0.8.

Our results suggest that small regions of the bed with prograde bed slope (here, this is defined as regions smaller than twice the seasonal swing in terminus position) are not sufficient to stop a retreating terminus. For example, at progressive retreat onset, the terminus of UMI was grounded on a sill with a retrograde bed slope of ~ −5°. During retreat, the bed slope shallowed but remained retrograde with the exception of one small region with prograde bed slope at a distance of 2,800 m along the centerline (Figure 4). However, this region is just a few hundred meters wide, roughly the same scale as seasonal changes in the UMI terminus (Table 2) and the terminus did not stabilize at this location during its retreat. Instead, UMI continued to retreat until it reached a more extensive (~1 km long) region of prograde bed slope (Figure 4). We see similar observations for other glaciers, and so we compute the overdeepening length, a measure of the length that bed slope remains retrograde, for all glaciers excluding small regions of the bed where the slope is prograde for lengths shorter than twice the typical seasonal amplitude of the terminus position (Table 2). We then compare the measured overdeepening length to the observed total amount of retreat observed since progressive retreat onset and find good agreement for all glaciers with well-constrained bed data in MCBed and poor fit for some glaciers where the MCBed is not as well constrained (Figure 5).

In a few cases, fjord geometry cannot explain all of the observed variability in terminus position. For example, KAN underwent a large retreat between 1998 and 2011 but has since stabilized despite its terminus being grounded in a deep portion of the fjord with a retrograde bed slope. This is why KAN plots below the 1:1 line on Figure 5. Rignot, Xu, et al. (2016) suggested that the stability of KAN is due to enhanced ice flux during retreat that began to exceed their modeled terminus melt rate in 2009. This is supported by our observation of sustained high velocities for KAN despite a stable terminus since 2010. KAN also is currently pinned in a region of the fjord with a small narrowing, which may also contribute to its stability. Rignot, Xu, et al. (2016) also found that RNK and KAS had ice fluxes that were much higher than terminus melt, which helps to stabilize their termini against retreat. We find that the fjord geometry for RNK and KAS further stabilizes them against retreat because in both cases the terminus is grounded downstream of topographic sills.

We also see that small, narrow overdeepenings restricted to the central portions of fjords can have an impact on glacier retreat by producing enhanced retreat in the deepest part of the fjord, likely because of focusing of subglacial water discharge within the overdeepening at the grounding line. Subglacial conduits enhance retreat due to melt and undercutting, which promotes calving (Fried et al., 2015). For example, KSS has a narrow overdeepening in the center of its fjord (spanning only 600 m of the 3.75-km-wide fjord, or just 16%) and extending only ~3 km along the fjord. Terminus retreat was enhanced in this overdeepening and led the entire terminus to retreat with it (supporting information Movie S3). As described by Lüthi et al. (2016), EQI has two overdeepenings within its fjord separated by a central ~110-m-tall bed bump that spans ~500 m. Enhanced retreat occurred in the location of each of the overdeepened regions, but the terminus remained pinned at the central bump until sufficient retreat occurred on either side of it to eventually pull the terminus off of the bump in 2013 (Lüthi et al., 2016; supporting information Movie S2).

In addition, locally enhanced retreat rates in the central portion of a terminus imparts changes in terminus shape through time as is observed for many glaciers. Thus, we suggest that the shape of the terminus may be diagnostic of the underlying processes controlling it. Convex termini are common where/when the terminus is well grounded on a sill (e.g., KAS) or central bed bump (e.g., EQI; supporting information Movie S2). Concave termini develop in regions where the fjord is overdeepened (e.g., KSS from 2005 to 2010). Many glaciers experience a change in terminus shape through time as they retreat. KSS, RNK, SIL, KUJ, and KAN have all gone from being convex at progressive retreat onset to more concave or flat as the termini retreated off of sills and into overdeepenings. Other glaciers (LIK and EQI) have termini that became more convex through time as the terminus retreated through portions of the fjord with bed bumps (supporting informaton figures).

4.4. Future Retreat

Our observations provide an opportunity to gauge future retreat of glaciers in our region given the context of past changes and improved mapping of the fjord geometry upstream of current termini. Several glaciers (LIK, LIL, and EQI; supporting information figures) have 2016 grounding lines less than 70 m below sea level indicating that they will soon be retreating above sea level, decoupling them from the ocean-forced mechanism that initiated retreat. EQI does have a much deeper trough upstream of the bump it is currently terminating on and thus could possibly exhibit long-term retreat if the terminus can be forced to retreat over this bump. Felikson et al. (2017) found extensive inland thinning of glaciers in response to terminus perturbations in the same ROI, and so we suspect that once these glaciers retreat out of the ocean, their impact to sea level will be minimized both due to reduced retreat rates but also due to slowed thinning rates.

Many of the glaciers in the ROI (KNG, KAS, STR, KSS, KUJ, RNK, UMI, PRD, and KAN) are presently stable or are likely to stabilize soon owing to fjord constrictions and prograde bed slopes immediately upstream from the 2016 terminus (supporting information figures). This suggestion was already postulated by Morlighem et al. (2016) for STR based on amplifying terminus losses to abnormally large values in order to force a retreat for this glacier. Since many glaciers have overdeepened beds behind these fjord constrictions, future retreat remains possible given enough of a perturbation to the terminus. To gauge this, we use our metric for the overdeepening length to estimate future retreat by searching upstream from the 2016 terminus position for the next possible stable terminus position (given as the blue square in Figure 3 and supplementary information figures). This suggests that ING, UMI, SIL, and KAN have the ability to retreat more than 1 km inland from their 2016 terminus positions (supporting information figures). Given that inland thinning as a result of these changes in terminus positions is already underway (Felikson et al., 2017), additional retreat is likely to force even more mass loss for these glaciers in the future.

5. Conclusions

We find near-synchronous progressive retreat onset in the late 1990s across a region of glaciers in central west Greenland that spans ~3° of latitude (roughly 250 km). Retreat often initiates in overdeepened portions of the bed where subglacial discharge is likely to be concentrated. The synchroneity and pattern of retreat onset suggest that increases in regional ocean and air temperatures acted together to amplify submarine melt at the terminus of glaciers across the region. While changes in runoff and ocean temperatures pushed the glaciers into a new state, the fjord topography is largely responsible for modulating the response to climate. Great progress has been made to model an evolving terminus face (Morlighem et al., 2016), yet these models parameterize uniform melt across the glacier terminus if the bed is below some depth (generally, if the bed is below 300 m, melt is applied along the entire column). Our observations suggest that focused melt associated with discrete subglacial discharge outlets may more accurately reproduce observations of terminus retreat in ice sheet models.

Total amounts of retreat are closely tied to the length of overdeepening behind the terminus at progressive retreat onset, which is heterogeneous across the region. This provides an explanation for previous studies who found great variability in retreat rate and durations between neighboring glaciers (e.g., Carr et al., 2017; Moon et al., 2015; Murray et al., 2015; Walsh et al., 2012). Assuming that the distance retreated is strongly controlled by the available length of retrograde bed slope, several glaciers in our study could experience additional retreat. These results suggest that observations of the fjord geometry immediately upstream of retreating glacier termini are critical in order to assess the future state of the Greenland Ice Sheet. These regions are often poorly observed in ice-penetrating radar surveys or sparsely surveyed with multibeam in the fjord immediately seaward of the terminus, and so we rely on mass-conservation techniques to improve our understanding of the bed. This is true for SIL (no radar data along flow to constrain MCBed) and ING (no multibeam downstream of the terminus). As a result, these glaciers, which are experiencing some of the largest amounts of retreat, are poorly understood in the context of this work. In addition, it is known that sediment deposition and erosion plays a key role in stabilizing fjord geometry against retreat (Brinkerhoff et al., 2017; Morlighem et al., 2016; Nick et al., 2007) and protecting grounding lines from deep, warm ocean water (Bartholomaus et al., 2013). Because we highlight the bed slope and fjord topography as critical controls on terminus dynamics, it may be pertinent to gain greater understanding of the rates of these processes in Greenland.

Acknowledgments
This work was supported by NASA (grant NNX12AP50G) and in part by the John A. and Katherine G. Jackson School of Geosciences at the University of Texas at Austin. We thank C. Black, A. Garcia, D. Peters, and G. Hsu for assisting with tracing of glacier termini. Mass-conserving bed data and some velocity data are available on the National Snow and Ice Data Center website. All other data used in this study are available at www.catania-ice.org/research and will be submitted to NSIDC upon publication of this manuscript. Finally, we thank the thorough and constructive review conducted by A. Vieli, an anonymous reviewer, and the Editor B. Hubbard, which significantly improved the manuscript.

References

Aniya, M., Sato, H., Naruse, R., Skvarca, P., & Casassa, G. (1997). Recent glacier variations in the Southern Patagonia Icefield, South America. *Arctic and Alpine Research*, *29*(1), 1–12. https://doi.org/10.2307/1551831

Bartholomaus, T. C., Larsen, C. F., & O'Neel, S. (2013). Does calving matter? Evidence for significant submarine melt. *Earth and Planetary Science Letters*, *380*, 21–30. https://doi.org/10.1016/j.epsl.2013.08.014

Bartholomaus, T. C., Stearns, L. A., Sutherland, D. A., Shroyer, E. L., Nash, J. D., Walker, R. T., et al. (2016). Contrasts in the response of adjacent fjords and glaciers to ice-sheet surface melt in West Greenland. *Annals of Glaciology*, *57*(73), 1–14. https://doi.org/10.1017/aog.2016.19

Bassis, J. N. (2013). Diverse calving patterns linked to glacier geometry. *Nature Geoscience*, *6*(10), 833–836. https://doi.org/10.1038/ngeo1887

Benn, D. I., Warren, C. R., & Mottram, R. H. (2007). Calving processes and the dynamics of calving glaciers. *Earth Science Reviews*, *82*(3), 143–179. https://doi.org/10.1016/j.earscirev.2007.02.002

Bevan, S. L., Luckman, A. J., Khan, S. A., & Murray, T. (2015). Seasonal dynamic thinning at Helheim Glacier. *Earth and Planetary Science Letters*, *415*, 47–53. https://doi.org/10.1016/j.epsl.2015.01.031

Bevan, S. L., Luckman, A. J., & Murray, T. (2012). Glacier dynamics over the last quarter of a century at Helheim, Kangerdlugssuaq and 14 other major Greenland outlet glaciers. *The Cryosphere*, *6*(5), 923–937. https://doi.org/10.5194/tc-6-923-2012

Bjørk, A. A., Kjær, K. H., Korsgaard, N. J., Khan, S. A., Kjeldsen, K. K., Andresen, C. S., et al. (2012). An aerial view of 80 years of climate-related glacier fluctuations in southeast Greenland. *Nature Geoscience*, *5*(6), 427–432. https://doi.org/10.1038/ngeo1481

Błaszczyk, M., Jania, J. A., & Kolondra, L. (2013). Fluctuations of tidewater glaciers in Hornsund Fjord (Southern Svalbard) since the beginning of the 20th century. *Polish Polar Research*, *34*(4), 327–352. https://doi.org/10.2478/popore-2013-0024

Brinkerhoff, D., Truffer, M., & Aschwanden, A. (2017). Sediment transport drives tidewater glacier periodicity. *Nature Communications*, *8*(1), 91. https://doi.org/10.1038/s41467-017-00095-5

Carr, J. R., Bell, H., Killick, R., & Holt, T. (2017). Exceptional retreat of Novaya Zemlya's marine-terminating outlet glaciers between 2000 and 2013. *The Cryosphere*, *11*(5), 2149–2174. https://doi.org/10.5194/tc-11-2149-2017

Carr, J. R., Stokes, C. R., & Vieli, A. (2013). Recent progress in understanding marine-terminating Arctic outlet glacier response to climatic and oceanic forcing: Twenty years of rapid change. *Progress in Physical Geography*, *37*(4), 436–467. https://doi.org/10.1177/0309133313483163

Carr, J. R., Stokes, C. R., & Vieli, A. (2014). Recent retreat of major outlet glaciers on Novaya Zemlya, Russian Arctic, influenced by fjord geometry and sea-ice conditions. *Journal of Glaciology*, *60*(219), 155–170. https://doi.org/10.3189/2014JoG13J122

Carr, J. R., Vieli, A., & Stokes, C. R. (2013). Influence of sea ice decline, atmospheric warming, and glacier width on marine-terminating outlet glacier behavior in northwest Greenland at seasonal to interannual timescales. *Journal of Geophysical Research: Earth Surface*, *118*(3), 1210–1226. https://doi.org/10.1002/jgrf.20088

Carr, J. R., Vieli, A., Stokes, C. R., Jamieson, S. S. R., Palmer, S. J., Christoffersen, P., et al. (2015). Basal topographic controls on rapid retreat of Humboldt Glacier, Northern Greenland. *Journal of Glaciology*, *61*(225), 137–150. https://doi.org/10.3189/2015JoG14J128

Carroll, D., Sutherland, D. A., Hudson, B., Moon, T., Catania, G. A., Shroyer, E. L., et al. (2016). The impact of glacier geometry on meltwater plume structure and submarine melt in Greenland fjords. *Geophysical Research Letters*, *43*, 9739–9748. https://doi.org/10.1002/2016GL070170

Cassotto, R., Fahnestock, M. A., Amundson, J. M., Truffer, M., & Joughin, I. R. (2015). Seasonal and interannual variations in ice melange and its impact on terminus stability, Jakobshavn isbræ, Greenland. *Journal of Glaciology*, *61*(225), 76–88. https://doi.org/10.3189/2015JoG13J235

Chauché, N., Hubbard, A. L., Gascard, J. C., Box, J. E., Bates, R., Koppes, M. N., et al. (2014). Ice–ocean interaction and calving front morphology at two west Greenland tidewater outlet glaciers. *The Cryosphere*, *8*(4), 1457–1468. https://doi.org/10.5194/tc-8-1457-2014

Chen, J. L., Wilson, C. R., & Tapley, B. D. (2011). Interannual variability of Greenland ice losses from satellite gravimetry. *Journal of Geophysical Research*, *116*, B07406. https://doi.org/10.1029/2010JB007789

Choi, Y., Morlighem, M., Rignot, E. J., Mouginot, J., & Wood, M. (2017). Modeling the response of Nioghalvfjerdsfjorden and Zachariae isstrøm Glaciers, Greenland, to ocean forcing over the next century. *Geophysical Research Letters*, *44*, 11,071–11,079. https://doi.org/10.1002/2017GL075174

Csatho, B. M., Schenk, A. F., van der Veen, C. J., Babonis, G. S., Duncan, K., Rezvanbehbahani, S., et al. (2014). Laser altimetry reveals complex pattern of Greenland Ice Sheet dynamics. *Proceedings of the National Academy of Sciences*, *111*(52), 18,478–18,483. https://doi.org/10.1073/pnas.1411680112

De Juan, J., Elósegui, P., Nettles, M., Larsen, T. B., Davis, J. L., Hamilton, G. S., et al. (2010). Sudden increase in tidal response linked to calving and acceleration at a large Greenland outlet glacier. *Geophysical Research Letters*, *37*, L12501. https://doi.org/10.1029/2010GL043289

Enderlin, E. M., Howat, I. M., & Vieli, A. (2013). High sensitivity of tidewater outlet glacier dynamics to shape. *The Cryosphere*, *7*(3), 1007–1015. https://doi.org/10.5194/tc-7-1007-2013

Fahnestock, M. A., Scambos, T. A., Moon, T., Gardner, A., Haran, T., & Klinger, M. (2016). Rapid large-area mapping of ice flow using Landsat 8. *Remote Sensing of Environment*, *185*, 84–94. https://doi.org/10.1016/j.rse.2015.11.023

Felikson, D., Bartholomaus, T. C., Catania, G. A., Korsgaard, N. J., Kjær, K. H., Morlighem, M., et al. (2017). Inland thinning on the Greenland ice sheet controlled by outlet glacier geometry. *Nature Geoscience*, *10*(5), 366–369. https://doi.org/10.1038/ngeo2934

Fried, M. J., Catania, G. A., Bartholomaus, T. C., Duncan, D., Davis, M., Stearns, L. A., et al. (2015). Distributed subglacial discharge drives significant submarine melt at a Greenland tidewater glacier. *Geophysical Research Letters*, *42*, 9328–9336. https://doi.org/10.1002/2015GL065806

Gladish, C. V., Holland, D. M., & Lee, C. M. (2015). Oceanic boundary conditions for Jakobshavn Glacier. Part II: Provenance and sources of variability of Disko Bay and Ilulissat Icefjord Waters, 1990–2011. *Journal of Physical Oceanography*, *45*(1), 33–63. https://doi.org/10.1175/JPO-D-14-0045.1

Holland, D. M., Thomas, R. H., De Young, B., Ribergaard, M. H., & Lyberth, B. (2008). Acceleration of Jakobshavn Isbræ triggered by warm subsurface ocean waters. *Nature Geoscience*, *1*(10), 659–664. https://doi.org/10.1038/ngeo316

Howat, I. M. (2017). *MEaSURES Greenland ice velocity: Selected glacier 660 site velocity maps from optical images, version 2*. Boulder, CO: NASA National 661 Snow and Ice Data Center Distributed Active Archive Center. https://doi.org/10.5067/VM5DZ20MYF5C

Howat, I. M., Box, J. E., Ahn, Y., Herrington, A., & McFadden, E. M. (2010). Seasonal variability in the dynamics of marine-terminating outlet glaciers in Greenland. *Journal of Glaciology*, *56*(198), 601–613.

Howat, I. M., Joughin, I. R., Tulaczyk, S. M., & Gogineni, S. P. (2005). Rapid retreat and acceleration of Helheim Glacier, east Greenland. *Geophysical Research Letters*, *32*, L22502. https://doi.org/10.1029/2005GL024737

Howat, I. M., Negrete, A., & Smith, B. E. (2014). The Greenland Ice Mapping Project (GIMP) land classification and surface elevation data sets. *The Cryosphere*, *8*(4), 1509–1518. https://doi.org/10.5194/tc-8-1509-2014

Jamieson, S. S. R., Vieli, A., Livingstone, S. J., O'Cofaigh, C., Stokes, C. R., Hillenbrand, C.-D., & Dowdeswell, J. A. (2012). Ice-stream stability on a reverse bed slope. *Nature Geoscience*, *5*(11), 799–802. https://doi.org/10.1038/ngeo1600

Jenkins, A. (2011). Convection-driven melting near the grounding lines of ice shelves and tidewater glaciers. *Journal of Physical Oceanography*, *41*(12), 2279–2294. https://doi.org/10.1175/JPO-D-11-03.1

Joughin, I. R., Howat, I. M., Fahnestock, M. A., Smith, B. E., Krabill, W. B., Alley, R. B., et al. (2008). Continued evolution of Jakobshavn Isbrae following its rapid speedup. *Journal of Geophysical Research*, *113*, F04006. https://doi.org/10.1029/2008JF001023

Joughin, I. R., Smith, B. E., Howat, I. M., Scambos, T. A., & Moon, T. (2010). Greenland flow variability from ice-sheet-wide velocity mapping. *Journal of Glaciology*, *56*(197), 415–430.

Larsen, S. H., Khan, S. A., Ahlstrøm, A. P., Hvidberg, C. S., Willis, M. J., & Andersen, S. B. (2016). Increased mass loss and asynchronous behavior of marine-terminating outlet glaciers at Upernavik Isstrøm, NW Greenland. *Journal of Geophysical Research: Earth Surface*, *121*, 241–256. https://doi.org/10.1002/2015JF003507

Lea, J. M., Mair, D. W. F., & Rea, B. R. (2017). Evaluation of existing and new methods of tracking glacier terminus change. *Journal of Glaciology*, *60*(220), 323–332. https://doi.org/10.3189/2014JoG13J061

Luckman, A. J., Murray, T., De Lange, R., & Hanna, E. (2006). Rapid and synchronous ice-dynamic changes in East Greenland. *Geophysical Research Letters*, *33*, L03503. https://doi.org/10.1029/2005GL025428

Lüthi, M. P., Vieli, A., Moreau, L., Joughin, I. R., Reisser, M., Small, D., & Stober, M. (2016). A century of geometry and velocity evolution at Eqip Sermia, West Greenland. *Journal of Glaciology*, *62*(234), 640–654. https://doi.org/10.1017/jog.2016.38

McFadden, E. M., Howat, I. M., Joughin, I. R., Smith, B. E., & Ahn, Y. (2011). Changes in the dynamics of marine terminating outlet glaciers in west Greenland (2000–2009). *Journal of Geophysical Research*, *116*, F01005. https://doi.org/10.1029/2010JF001757

McNabb, R. W., & Hock, R. (2014). Alaska tidewater glacier terminus positions, 1948–2012. *Journal of Geophysical Research: Earth Surface*, *119*, 153–167. https://doi.org/10.1002/2013JF002915

Meier, M. F., & Post, A. (1987). Fast tidewater glaciers. *Journal of Geophysical Research*, *92*(B9), 9051–9058.

Mercer, J. H. (1961). The response of fjord glaciers to changes in the firn limit. *Journal of Glaciology*, *3*(29), 850–858.

Mernild, S. H., Mote, T. L., & Liston, G. E. (2011). Greenland ice sheet surface melt extent and trends: 1960-2010. *Journal of Glaciology*, *57*(204), 621–628.

Moon, T., & Joughin, I. R. (2008). Changes in ice front position on Greenland's outlet glaciers from 1992 to 2007. *Journal of Geophysical Research*, *113*, F02022. https://doi.org/10.1029/2007JF000927

Moon, T., Joughin, I. R., & Smith, B. E. (2015). Seasonal to multiyear variability of glacier surface velocity, terminus position, and sea ice/ice mélange in northwest Greenland. *Journal of Geophysical Research: Earth Surface*, *120*, 818–833. https://doi.org/10.1002/2015JF003494

Moon, T., Joughin, I. R., Smith, B. E., & Howat, I. M. (2012). 21st-century evolution of greenland outlet glacier velocities. *Science*, *336*(6081), 576–578. https://doi.org/10.1126/science.1219985

Morlighem, M., Bondzio, J. H., Seroussi, H., Rignot, E. J., Larour, E. Y., Humbert, A., & Rebuffi, S. (2016). Modeling of Store Gletscher's calving dynamics, West Greenland, in response to ocean thermal forcing. *Geophysical Research Letters*, *43*, 2659–2666. https://doi.org/10.1002/2016GL067695

Morlighem, M., Williams, C. N., Rignot, E. J., An, L., Arndt, J. E., Bamber, J. L., et al. (2017). Bedmachine v3: Complete bed topography and ocean Bathymetry mapping of greenland from multibeam echo sounding combined with mass conservation. *Geophysical Research Letters*, *44*, 11,051–11,061. https://doi.org/10.1002/2017GL074954

Motyka, R. J., Cassotto, R., Truffer, M., Kjeldsen, K. K., van As, D., Korsgaard, N. J., et al. (2017). Asynchronous behavior of outlet glaciers feeding Godthåbsfjord (Nuup Kangerlua) and the triggering of Narsap Sermia's retreat in SW Greenland. *Journal of Glaciology*, *63*(238), 288–308. https://doi.org/10.1017/jog.2016.138

Motyka, R. J., Hunter, L. E., Echelmeyer, K. A., & Connor, C. (2003). Submarine melting at the terminus of a temperate tidewater glacier, LeConte Glacier, Alaska, U.S.A. *Annals of Glaciology*, *36*, 57–65.

Motyka, R. J., Truffer, M., Fahnestock, M. A., Mortensen, J., Rysgaard, S., & Howat, I. M. (2011). Submarine melting of the 1985 Jakobshavn Isbrae floating tongue and the triggering of the current retreat. *Journal of Geophysical Research*, *116*, F01007. https://doi.org/10.1029/2009JF001632

Murray, T., Scharrer, K., Selmes, N., Booth, A. D., James, T. D., Bevan, S. L., et al. (2015). Extensive retreat of Greenland tidewater glaciers, 2000–2010. *Arctic Antarctic And Alpine Research*, *47*(3), 427–447. https://doi.org/10.1657/AAAR0014-049

Myers, P. G., & Ribergaard, M. H. (2013). Warming of the polar water layer in disko bay and potential impact on Jakobshavn Isbrae. *Journal of Physical Oceanography*, *43*(12), 2629–2640. https://doi.org/10.1175/JPO-D-12-051.1

Nick, F. M., van der Veen, C. J., & Oerlemans, J. (2007). Controls on advance of tidewater glaciers: Results from numerical modeling applied to columbia glacier. *Journal of Geophysical Research*, *112*, F03S24. https://doi.org/10.1029/2006JF000551

Nick, F. M., van der Veen, C. J., & Vieli, A. (2010). A physically based calving model applied to marine outlet glaciers and implications for the glacier dynamics. *Journal of Glaciology*, *56*(199), 781–794.

Nick, F. M., Vieli, A., Howat, I. M., & Joughin, I. R. (2009). Large-scale changes in Greenland outlet glacier dynamics triggered at the terminus. *Nature Geoscience*, *2*(2), 110–114. https://doi.org/10.1038/ngeo394

Nöel, B., van De Berg, W. J., Lhermitte, S., Wouters, B., Machguth, H., Howat, I. M., et al. (2017). A tipping point in refreezing accelerates mass loss of Greenland's glaciers and ice caps. *Nature Communications*, *8*, 14730. https://doi.org/10.1038/ncomms14730

Pfeffer, W. T. (2007). A simple mechanism for irreversible tidewater glacier retreat. *Journal of Geophysical Research*, *112*, F03S25. https://doi.org/10.1029/2006JF000590

Post, A., O'Neel, S., Motyka, R. J., & Streveler, G. (2011). A complex relationship between calving glaciers and climate. *Eos, Transactions American Geophysical Union*, *92*(37), 305–306.

Rignot, E. J., Fenty, I., Xu, Y., Cai, C., Velicogna, I., O'Cofaigh, C., et al. (2016). Bathymetry data reveal glaciers vulnerable to ice-ocean interaction in Uummannaq and Vaigat glacial fjords, West Greenland. *Geophysical Research Letters*, *43*(6), 2667–2674. https://doi.org/10.1002/2016GL067832

Rignot, E. J., Xu, Y., Menemenlis, D., Mouginot, J., Scheuchl, B., Li, X., et al. (2016). Modeling of ocean-induced ice melt rates of five west Greenland glaciers over the past two decades. *Geophysical Research Letters*, *43*(12), 6374–6382. https://doi.org/10.1002/2016GL068784

Robel, A. A. (2017). Thinning sea ice weakens buttressing force of iceberg mélange and promotes calving. *Nature Communications*, *8*, 14596. https://doi.org/10.1038/ncomms14596

Rosenau, R., Scheinert, M., & Dietrich, R. (2015). A processing system to monitor Greenland outlet glacier velocity variations at decadal and seasonal time scales utilizing the Landsat imagery. *Remote Sensing of Environment*, *169*, 1–19. https://doi.org/10.1016/j.rse.2015.07.012

Schild, K. M., & Hamilton, G. S. (2013). Seasonal variations of outlet glacier terminus position in Greenland. *Journal of Glaciology*, *59*(216), 759–770. https://doi.org/10.3189/2013JoG12J238

Schoof, C. G. (2007). Ice sheet grounding line dynamics: Steady states, stability, and hysteresis. *Journal of Geophysical Research*, *112*, F03S28. https://doi.org/10.1029/2006JF000664

Seroussi, H., Nakayama, Y., Larour, E. Y., Menemenlis, D., Morlighem, M., Rignot, E. J., & Khazendar, A. (2017). Continued retreat of Thwaites Glacier, West Antarctica, controlled by bed topography and ocean circulation. *Geophysical Research Letters*, *44*, 6191–6199. https://doi.org/10.1002/2017GL072910

Straneo, F., Hamilton, G. S., Sutherland, D. A., Stearns, L. A., Davidson, F. J. M., Hammill, M. O., et al. (2010). Rapid circulation of warm subtropical waters in a major glacial fjord in East Greenland. *Nature Geoscience*, *3*(3), 182–186. https://doi.org/10.1038/ngeo764

Straneo, F., & Heimbach, P. (2013). North Atlantic warming and the retreat of Greenland's outlet glaciers. *Nature*, *504*(7478), 36–43. https://doi.org/10.1038/nature12854

Studinger, M., Koenig, L., Martin, S., & Sonntag, J. (2010). Operation icebridge: Using instrumented aircraft to bridge the observational gap between icesat and icesat-2. In *IGARSS 2010 - 2010 IEEE International Geoscience and Remote Sensing Symposium* (pp. 1918–1919). IEEE, Honolulu, HI. https://doi.org/10.1109/IGARSS.2010.5650555

Thomas, R. H., Abdalati, W., Friderick, E., Krabill, W. B., Manizade, S., & Steffen, K. (2003). Investigation of surface melting and dynamic thinning on Jakobshavn Isbrae, Greenland. *Journal of Glaciology*, *49*(165), 231–239.

Thomas, R. H., & Bentley, C. R. (1978). A model for holocene retreat of the west antarctic ice sheet. *Quaternary Research*, *10*(2), 150–170. https://doi.org/10.1016/0033-5894(78)90098-4

van Angelen, J. H., van den Broeke, M. R., Wouters, B., & Lenaerts, J. T. M. (2014). Contemporary (1960–2012) evolution of the climate and surface mass balance of the Greenland ice sheet. *Surveys in Geophysics*, *35*(5), 1155–1174. https://doi.org/10.1007/s10712-013-9261-z

van der Veen, C. J. (1996). Tidewater calving. *Journal of Glaciology*, *42*(141), 375–385.

van der Veen, C. J., Plummer, J., & Stearns, L. A. (2011). Controls on the recent speed-up of Jakobshavn Isbrae, West Greenland. *Journal of Glaciology*, *57*(204), 770–782.

Velicogna, I., Sutterley, T. C., & van den Broeke, M. R. (2014). Regional acceleration in ice mass loss from Greenland and Antarctica using GRACE time-variable gravity data. *Geophysical Research Letters*, *41*, 8130–8137. https://doi.org/10.1002/2014GL061052

Walsh, K. M., Howat, I. M., Ahn, Y., & Enderlin, E. M. (2012). Changes in the marine-terminating glaciers of central east Greenland, 2000–2010. *The Cryosphere*, *6*(1), 211–220. https://doi.org/10.5194/tc-6-211-2012

Warren, C. R. (1991). Terminal environment, topographic control and fluctuations of West Greenland glaciers. *Boreas*, *20*(1), 1–15. https://doi.org/10.1111/j.1502-3885.1991.tb00453.x

Warren, C. R., & Glasser, N. F. (1992). Contrasting response of south Greenland glaciers to recent climatic change. *Arctic and Alpine Research*, *24*(2), 124–132.

Weertman, J. (1974). Stability of the junction of an ice sheet and an ice shelf. *Journal of Glaciology*, *13*(67), 3–11.